inorganics

MDPI

Supplementary Materials: Investigating the Factors Affecting the Ionic Conduction in Nanoconfined $NaBH_4$

Xiaoxuan Luo, Aditya Rawal, and Kondo-Francois Aguey-Zinsou

Citation: Luo, X.; Rawal, A.; Aguey-Zinsou, K.-F. Investigating the Factors Affecting the Ionic Conduction in Nanoconfined $NaBH_4$. *Inorganics* **2021**, *9*, 2. https://doi.org/10.3390/inorganics9010002

Received: 28 November 2020
Accepted: 23 December 2020
Published: 8 January 2021

Table 1. Summary of BET analysis for MCM-41, $NaBH_4$@MCM-41 and $LiBH_4$@MCM-41.

Sample	Total pore volume ($cm^3\ g^{-1}$)	BET surface area ($m^2\ g^{-1}$)
MCM-41	1.02	1110.91
$LiBH_4$@MCM-41	0.03	14.38
$NaBH_4$@MCM-41	0.02	3.5

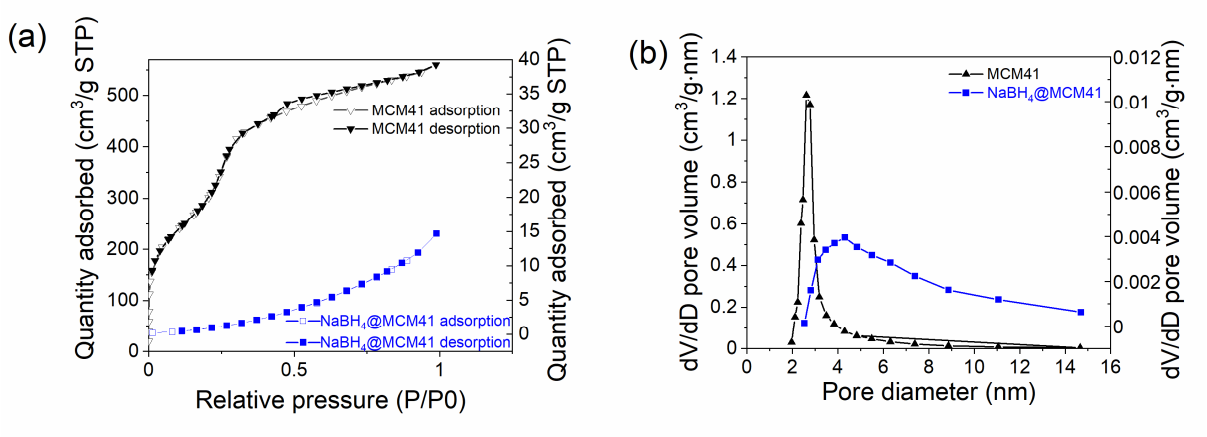

Figure S1. BET analysis for MCM-41 and $NaBH_4$@MCM-41: (a) N_2 physisorption and (b) pore size distribution.

MCM-41 shows a type IV isotherm, which confirms that MCM-41 is a mesoporous material [1]. After melt infiltration, the isotherm became of type II. This implies that the material is non-porous and of macroporous type [2].

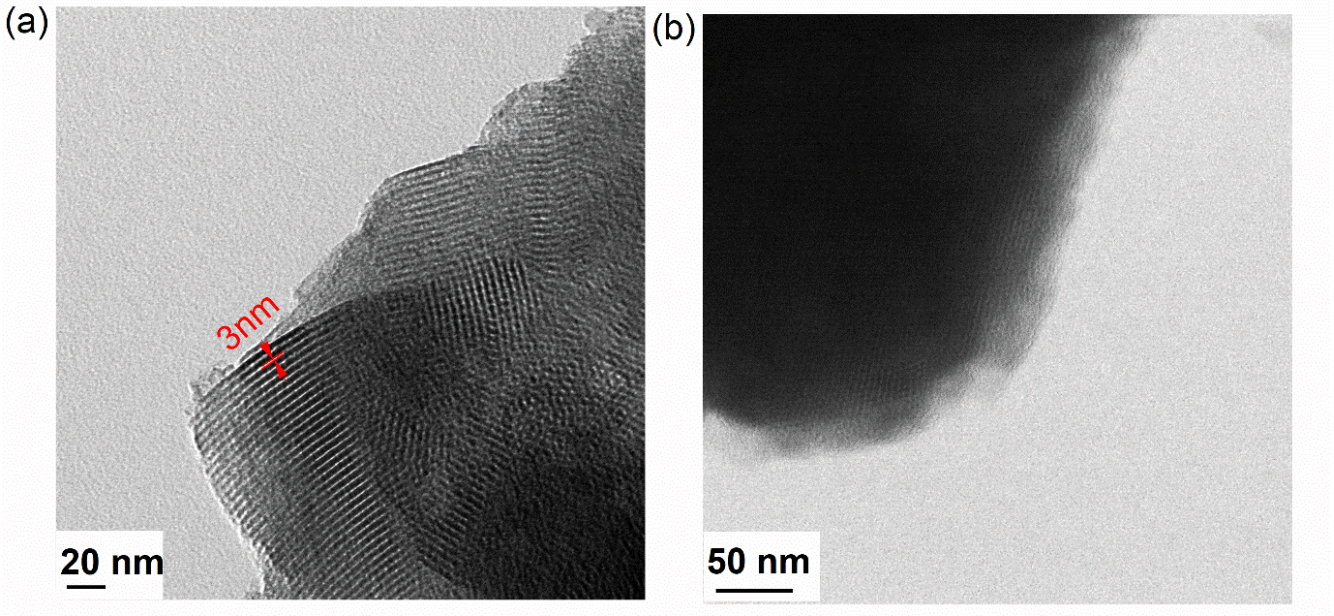

Figure S2. Typical TEM image of (a) the empty scaffold MCM-41, and (b) $NaBH_4$@MCM-41.

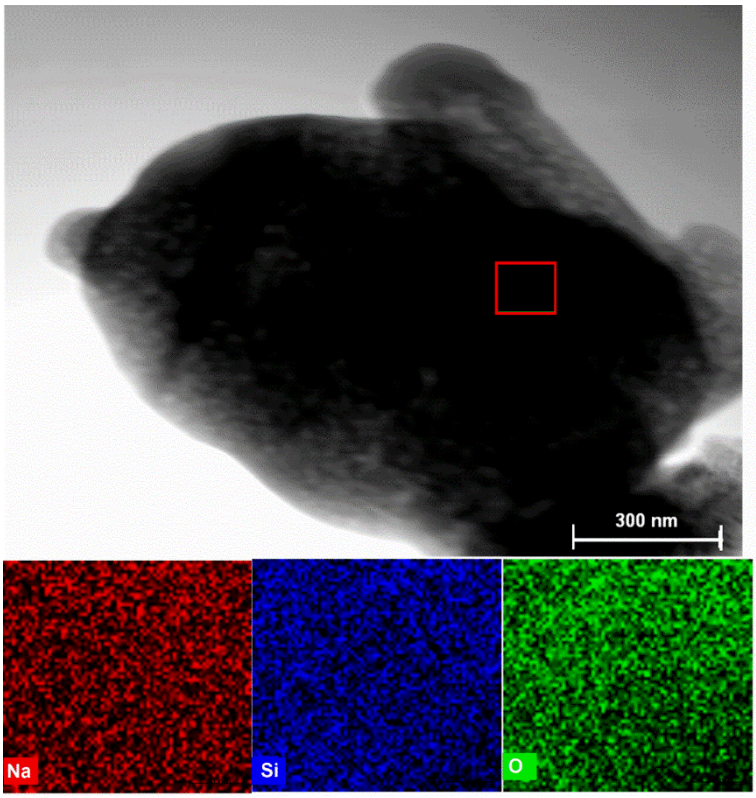

Figure S3. STEM elemental mapping of $NaBH_4$@MCM-41.

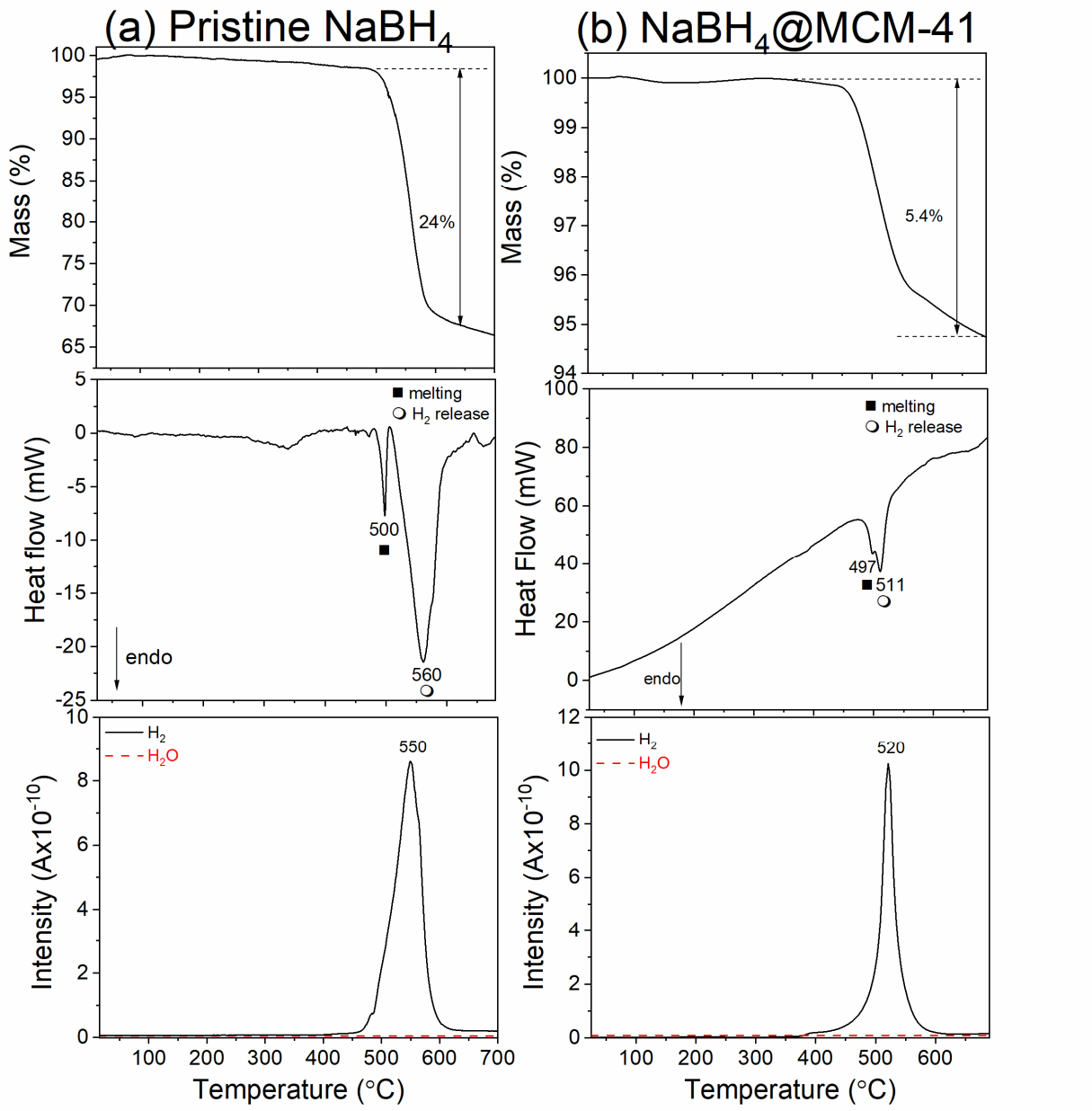

Figure S4. TGA-DSC-MS profiles of (a) pristine $NaBH_4$ and (b) $NaBH_4$@MCM-41.

The excessive mass loss of pristine $NaBH_4$ is due to Na evaporation. The BET results indicated that the pores of the MCM-41 were filled at 78 %. The corresponding mass loss observed by TGA should be of 5.1 instead of 5.4%. The excess (0.3%) may be due to the evaporation of Na upon the melting of $NaBH_4$.

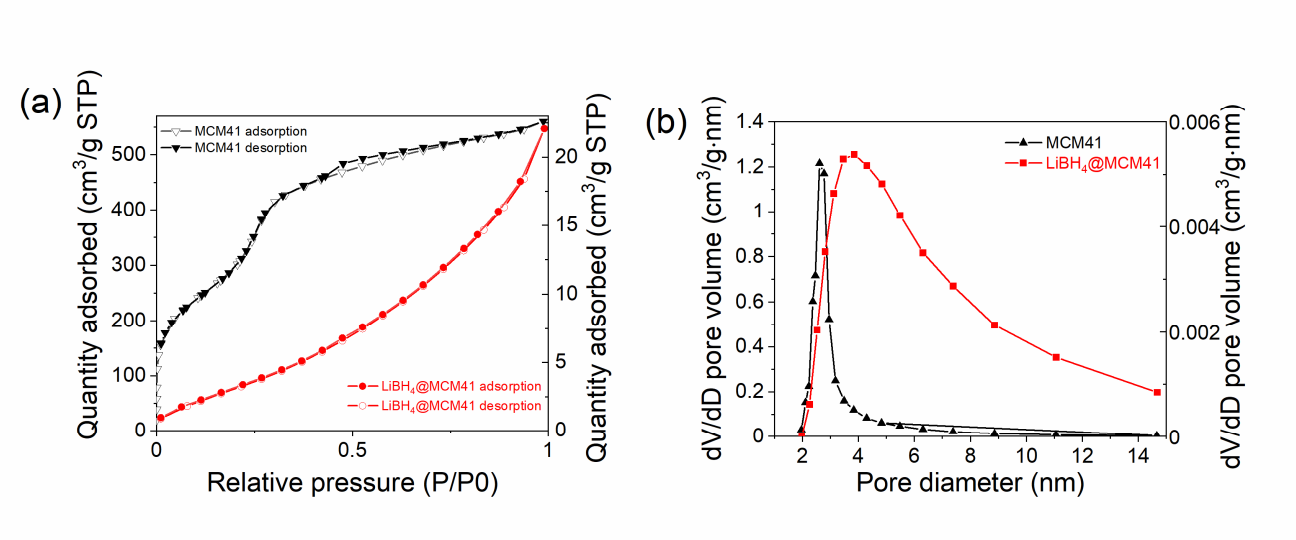

Figure S5. BET analysis for MCM-41 and $LiBH_4$@MCM-41: (a) N_2-physisorption, and (b) pore size distribution.

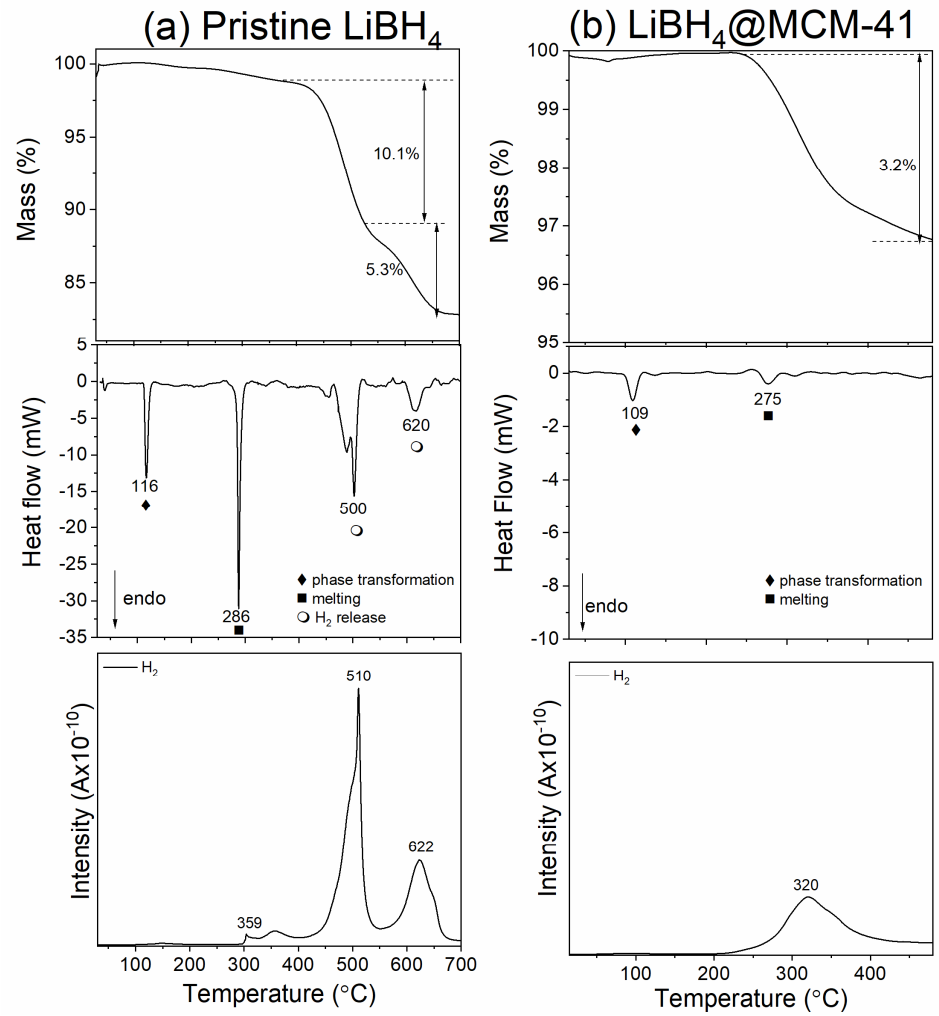

Figure S6. TGA-DSC-MS profiles of (a) pristine $LiBH_4$ and (b) $LiBH_4$@MCM-41.

The endothermic peak observed by DSC at 116 °C for pristine $LiBH_4$ was assigned to the phase transition from orthorhombic (Pnma) to hexagonal (P63mc) $LiBH_4$. At 286 °C, the melting of $LiBH_4$ was also observed, in agreement with the literature [3]. Upon nano-confinement of $LiBH_4$, some a weak DSC signal related to the phase transition and melting

of $LiBH_4$ were still visible although at the lower temperatures of 109 and 275 °C, respectively. Fully nanoconfined $LiBH_4$ has been reported to show no DSC signal for the phase transition [4]. In the current work, this may be explained by the existence of some $LiBH_4$ outside the MCM-41 porosity, although yet to be confirmed because the hydrogen release profile only showed a single peak at 320 °C, which indicates a very well confined material, as per previous reports [5].

The 3.2 % mass loss observed upon nanoconfinement of $LiBH_4$ by TGA indicates that 73 % of $LiBH_4$ is confined in MCM-41 instead of the 83% indicated by BET analysis. The discrepancy may be due to the formation of by-products (i.e. oxides and $B_{12}H_{12}$ phase) during melt infiltration.

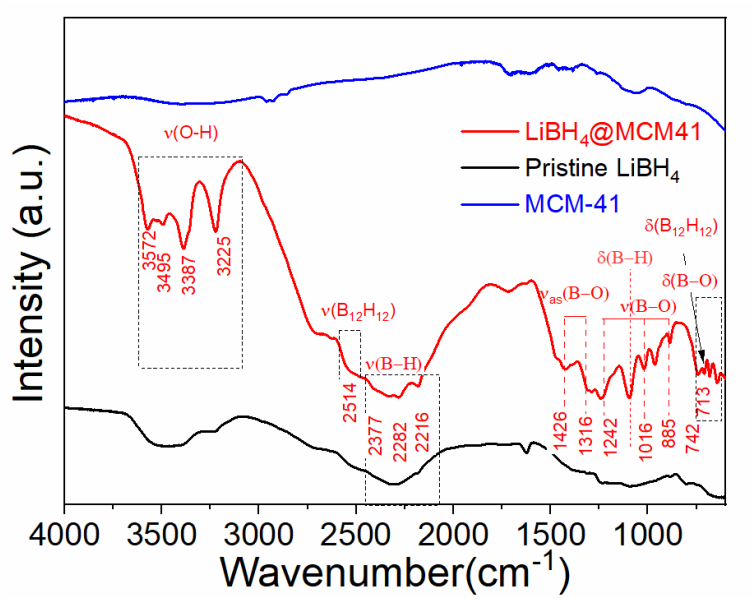

Figure S7. FTIR analysis of $LiBH_4$@MCM-41 and pristine $LiBH_4$.

Vibrations corresponding to four- and three-coordinated B-O were observed by FTIR analysis of nanoconfined $LiBH_4$ in MCM-41 and this indicated the presence of oxides phases [6]. In addition, the $B_{12}H_{12}$ vibration at 2514 cm^{-1} and 713 cm^{-1} were detected, corresponding to the $Li_2B_{12}H_{12}$ phase.[7,8] This can be attributed to the partial decomposition of $LiBH_4$.[9]

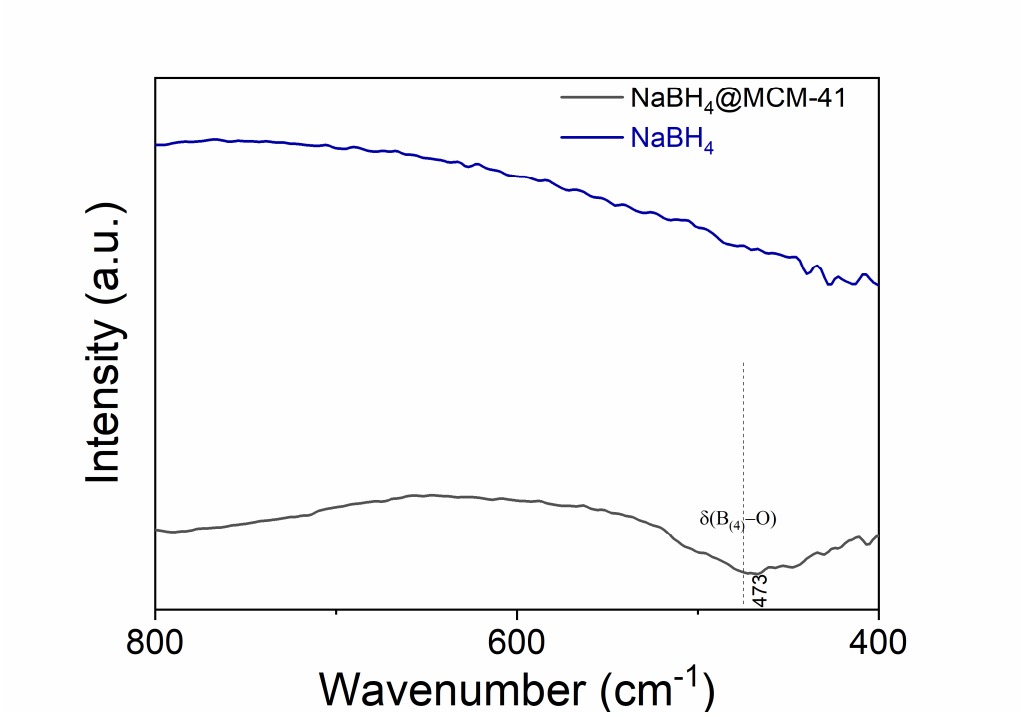

Figure S8. FTIR analysis of $NaBH_4$@MCM-41 and pristine $NaBH_4$.

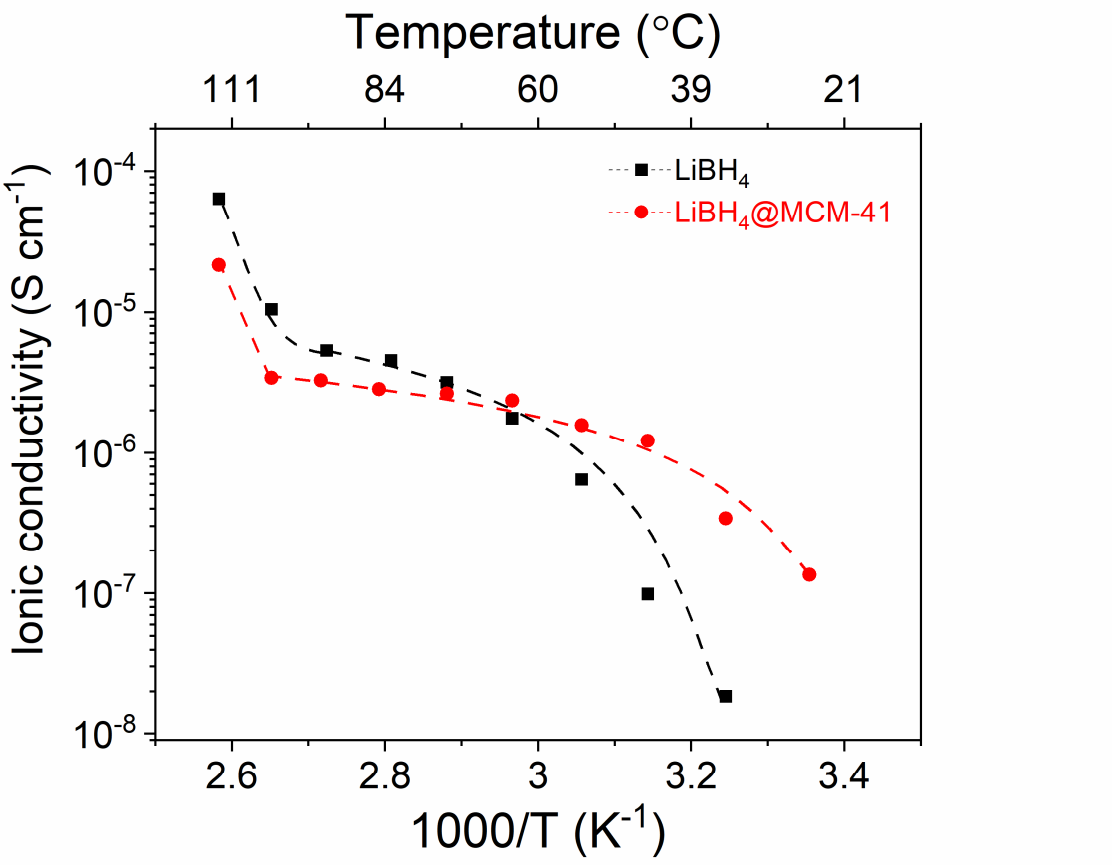

Figure S9. Arrhenius plot of $LiBH_4$@MCM-41 and pristine $LiBH_4$.

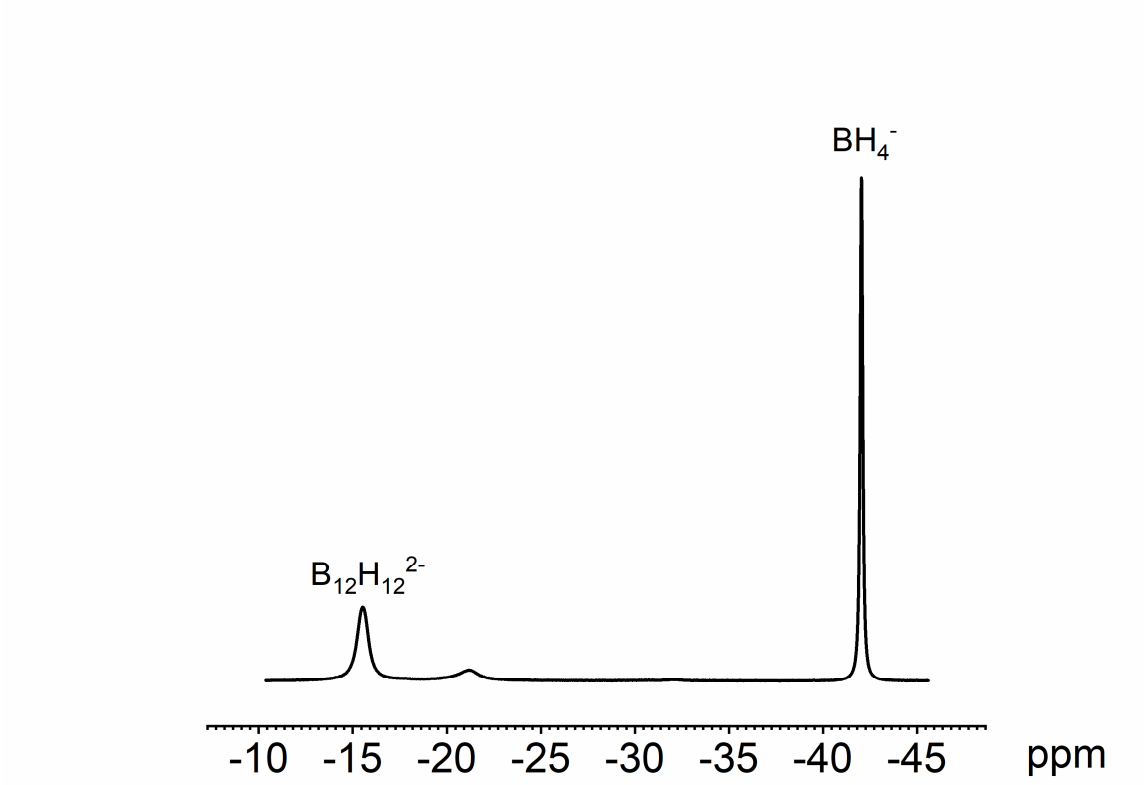

Figure S10. ^{11}B NMR of the $NaBH_4$ + $Na_2B_{12}H_{12}$ composite synthesised by exposing $NaBH_4$ to B_2H_6.

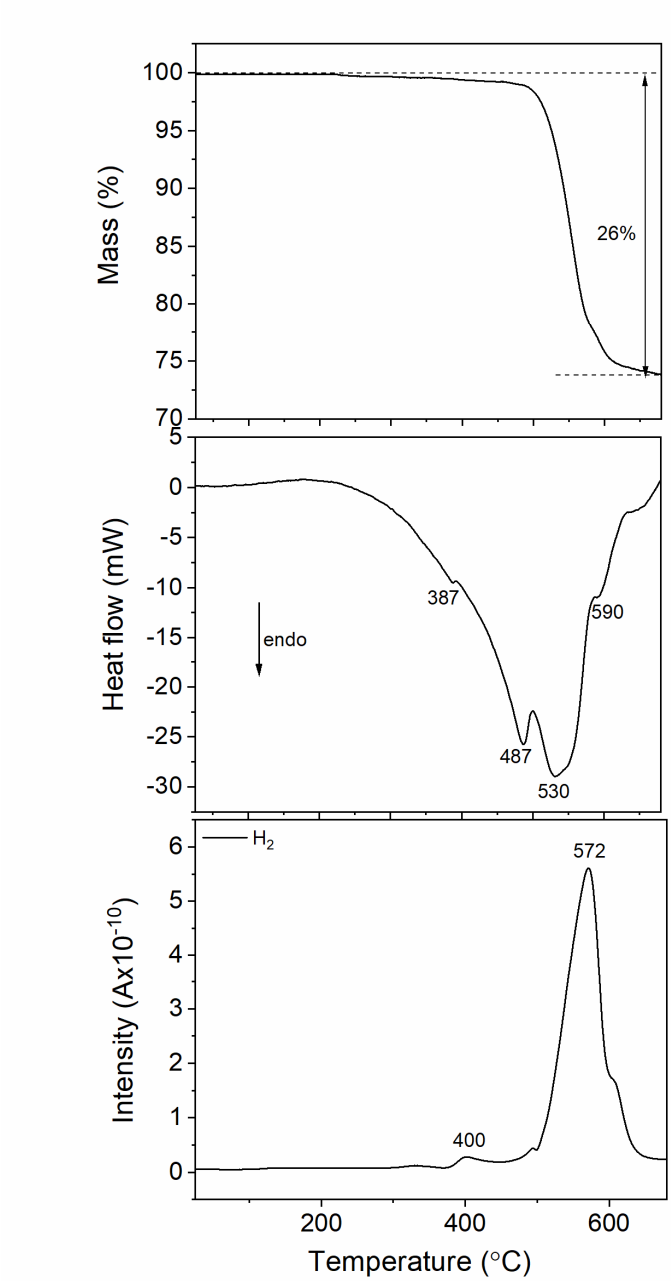

Figure S11. TGA-DSC MS of the $NaBH_4$+$Na_2B_{12}H_{12}$ composite synthesised by exposing $NaBH_4$ to B_2H_6.

References

1. Kruk, M.; Jaroniec, M.; Sayari, A. Adsorption Study of Surface and Structural Properties of MCM-41 Materials of Different Pore Sizes. *J. Phys. Chem. B* **1997**, *101*, 583–589, doi:10.1021/jp962000k.
2. Sing, K.S. Reporting physisorption data for gas/solid systems with special reference to the determination of surface area and porosity. *Pure Appl. Chem.* **1985**, *57*, 603–619.
3. Miwa, K.; Ohba, N.; Towata, S.-i.; Nakamori, Y.; Orimo, S.-i. First-principles study on lithium borohydride $LiBH_4$. *Phys. Rev. B* **2004**, *69*, 245120, doi:10.1103/PhysRevB.69.245120.
4. Wang, S.; Otomo, J.; Ogura, M.; Wen, C.-j.; Nagamoto, H.; Takahashi, H. Preparation and characterization of proton-conducting $CsHSO_4$–SiO_2 nanocomposite electrolyte membranes. *Solid State Ion.* **2005**, *176*, 755–760, doi:doi.org/10.1016/j.ssi.2004.10.013.
5. Cahen, S.; Eymery, J.B.; Janot, R.; Tarascon, J.M. Improvement of the $LiBH_4$ hydrogen desorption by inclusion into mesoporous carbons. *J. Power Sources* **2009**, *189*, 902–908, doi:doi.org/10.1016/j.jpowsour.2009.01.002.
6. Jun, L.; Shuping, X.; Shiyang, G. FT-IR and Raman spectroscopic study of hydrated borates. *Spectrochim. Acta, Part A* **1995**, *51*, 519–532, doi:doi.org/10.1016/0584-8539(94)00183-C.

7. Huang, Z.; Gallucci, J.; Chen, X.; Yisgedu, T.; Lingam, H.K.; Shore, S.G.; Zhao, J.-C. $Li_2B_{12}H_{12}{\cdot}NH_3$: a new ammine complex for ammonia storage or indirect hydrogen storage. *J. Mater. Chem.* **2010**, *20*, 2743, doi:10.1039/b923829h.
8. Geis, V.; Guttsche, K.; Knapp, C.; Scherer, H.; Uzun, R. Synthesis and characterization of synthetically useful salts of the weakly-coordinating dianion [B12Cl12]2−. *Dalton T.* **2009**, 2687–2694.
9. Ozolins, V.; Majzoub, E.H.; Wolverton, C. First-Principles Prediction of Thermodynamically Reversible Hydrogen Storage Reactions in the Li-Mg-Ca-B-H System. *J. Am. Chem. Soc.* **2009**, *131*, 230–237, doi:10.1021/ja8066429.